Acta Cryst E CRYSTALLOGRAPHIC COMMUNICATIONS
ISSN 2056-9890

Organic–inorganic hybrid hexachloridostannate(IV) with 2-methylimidazo[1,5-*a*]pyridin-2-ium cation

Olga Yu. Vassilyeva,[a]* Elena A. Buvaylo,[a] Vladimir N. Kokozay[a] and Alexandre N. Sobolev[b]

[a]Department of Chemistry, Taras Shevchenko National University of Kyiv, 64/13 Volodymyrska Street, Kyiv 01601, Ukraine, and [b]School of Molecular Sciences, M310, the University of Western Australia, 35 Stirling Highway, Perth, 6009, W.A., Australia. *Correspondence e-mail: vassilyeva@univ.kiev.ua

Received 12 December 2022
Accepted 11 January 2023

Edited by S. Parkin, University of Kentucky, USA

Keywords: crystal structure; hybrid salt; tin(IV); 2-pyridinecarbaldehyde.

CCDC reference: 2235690

Supporting information: this article has supporting information at journals.iucr.org/e

The hybrid salt bis(2-methylimidazo[1,5-*a*]pyridin-2-ium) hexachloridostannate(IV), $(C_8H_9N_2)_2[SnCl_6]$, crystallizes in the monoclinic space group $P2_1/n$ with the asymmetric unit containing an $Sn_{0.5}Cl_3$ fragment (Sn site symmetry $\overline{1}$) and one organic cation. The five- and six-membered rings in the cation are nearly coplanar; bond lengths in the pyridinium ring of the fused core are as expected; the C—N/C bond distances in the imidazolium entity fall in the range 1.337 (5)–1.401 (5) Å. The octahedral $SnCl_6^{2-}$ dianion is almost undistorted with the Sn–Cl distances varying from 2.4255 (9) to 2.4881 (8) Å and the *cis* Cl—Sn—Cl angles approaching 90°. In the crystal, π-stacked chains of cations and loosely packed $SnCl_6^{2-}$ dianions form separate sheets alternating parallel to (101). Most of the numerous C—H···Cl—Sn contacts between the organic and inorganic counterparts with the H···Cl distances above the van der Waals contact limit of 2.85 Å are considered a result of crystal packing.

1. Chemical context

Organic–inorganic hybrid perovskites that combine discrete organic cations and rigid metal halide architectures have been considered promising materials for diverse optoelectronic applications: solar cells, light-emitting diodes, photodetectors, spintronics (Gan *et al.*, 2021; Li *et al.*, 2021). Most of the materials reported to date are based on Pb^{II}, Sb^{III}, Bi^{III} and Cd^{II} halides (Saparov & Mitzi, 2016), whose widespread application is restrained by the potential toxicity. Being in the same main group of metal atoms that Pb belongs to, Sn forms hybrid halide perovskites with similar electronic properties, which are more friendly to the environment. At the same time, the aforementioned hybrid systems suffer from high water permeability and low thermal stability, the issues being largely related to the volatility of small organic cations (Leijtens *et al.*, 2015). The stability of hybrid perovskites can be improved by introducing larger organic cations and lowering the dimensionality of the octahedral halometallate frameworks (Zhang *et al.*, 2016; Leblanc *et al.*, 2019). Moreover, functional organic cations are a valuable tool for introducing useful properties into the hybrid structure. For example, the use of the photoactive zwitterion viologen *N*,*N*′-4,4′-bipyridiniodipropionate (CV) afforded the formation of the covalently bonded pillared layered bromoplumbate, $[Pb_3Br_6(CV)]_n$, showing high thermal stability in air and a remarkable increase of capacitance after photoinduced electron transfer (Sun *et al.*, 2019). Mono-periodic hybrid lead halides incorporating optically

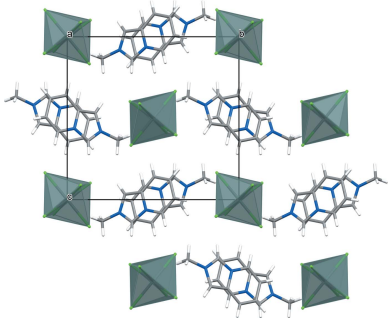

active protonated 1,3-bis(4-pyridyl)-propane cations exhibit dual-light emissions combined of higher energy blue and lower energy yellow light spectra, which were attributed to the individual contributions of the organic and inorganic components (Sun *et al.*, 2021).

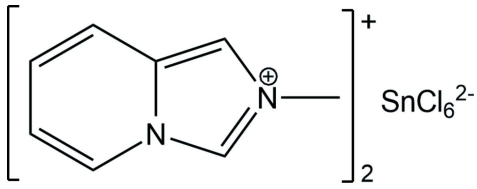

Multiple advantages of the organic–inorganic hybrid materials inspire the huge appeal in exploring other kinds of low-dimensional metal halide compounds templated by functional aromatic cations. Fine-tuning of the electronic structure and optoelectronic properties of the metal halide hybrids, which depend, among other things, on the anionic speciation and halogen ratio, can be achieved by mixing halide ligands in self-assembled organic–inorganic systems (Rogers *et al.*, 2019; Askar *et al.*, 2018).

Pursuing our research on hybrid halometalates incorporating substituted imidazo[1,5-*a*]pyridinium cations (Buvaylo *et al.*, 2015; Vassilyeva *et al.*, 2019; 2020; 2021), we attempted the synthesis of a hybrid tin mixed halide with 2-methylimidazo[1,5-*a*]pyridinium, L^+, a product of the oxidative cyclocondensation between 2-pyridinecarbaldehyde (2-PCA), formaldehyde and CH_3NH_2. One necessary component of the reaction is acid, which is introduced as a hydrohalide adduct of the amine (Vassilyeva *et al.*, 2020). Following the method of preparation used to obtain mixed-halide Zn^{II} and Cd^{II} tetrahalometalates (Cl/I, Br/Cl) with L^+ (Vassilyeva *et al.*, 2022), $SnCl_2{\cdot}2H_2O$ was reacted with the solution of L^+ formed *in situ* using 2-PCA, formaldehyde and $CH_3NH_2{\cdot}HBr$. The isolated product was crystallographically characterized as $[L]_2[SnCl_6]$, (I); the detrimental oxidation of Sn^{II} to Sn^{IV} appeared unavoidable leading to the formation of ubiquitous hexachloridostannate(IV) dianion. Herein, the synthesis, structural analysis and spectroscopic characterization of (I) are reported.

2. Structural commentary

The title hybrid salt, with formula $(C_8H_9N_2)_2[SnCl_6]$, crystallizes in the monoclinic space group $P2_1/n$. The asymmetric unit consists of an $Sn_{0.5}Cl_3$ fragment (Sn site symmetry $\overline{1}$) and 2-methylimidazo[1,5-*a*]pyridinium cation, as shown in Fig. 1. The structural configuration of the cation is similar to those of other 2-methylimidazo[1,5-*a*]pyridinium hybrid salts $(C_8H_9N_2)_2[ZnCl_4]$ (GOTHAB; Vassilyeva *et al.*, 2020) and $(C_8H_9N_2)_2[CdCl_4]$ (GOTJAD; Vassilyeva *et al.*, 2021). Bond lengths in the pyridinium ring of the fused core are as expected; the C—N/C bond distances in the imidazolium entity fall in the range 1.337 (5)–1.401 (5) Å; N2 and N3*A* atoms are planar with the sums of three angles being equal to 360°. The almost coplanar five- and six-membered rings in the cation show the dihedral angle between them of 1.6 (2)°. The octahedral $SnCl_6^{2-}$ dianion in (I) is almost undistorted with the Sn—Cl distances varying from 2.4255 (9) to 2.4881 (8) Å and the *cis* Cl—Sn—Cl angles approaching 90° (Table 1). The geometric parameters of the dianion are normal and comparable to those of similar structure types.

Table 1
Selected geometric parameters (Å, °).

Sn1—Cl1	2.4255 (9)	Sn1—Cl2	2.4881 (8)
Sn1—Cl3	2.4777 (8)		
$Cl1^i$—Sn1—Cl3	89.72 (3)	Cl3—Sn1—$Cl2^i$	90.59 (3)
Cl1—Sn1—Cl3	90.28 (3)	Cl1—Sn1—Cl2	89.80 (3)
Cl1—Sn1—$Cl2^i$	90.20 (3)	Cl3—Sn1—Cl2	89.41 (3)

Symmetry code: (i) $-x+1, -y+1, -z+1$.

3. Supramolecular features

In the crystal, cationic and anionic sheets alternate lying parallel to (101) (Fig. 2). In the sheets, pairs of centrosymmetically related *trans*-oriented L^+ cations demonstrate offset 10πe–10πe stacking with a centroid–centroid distance of

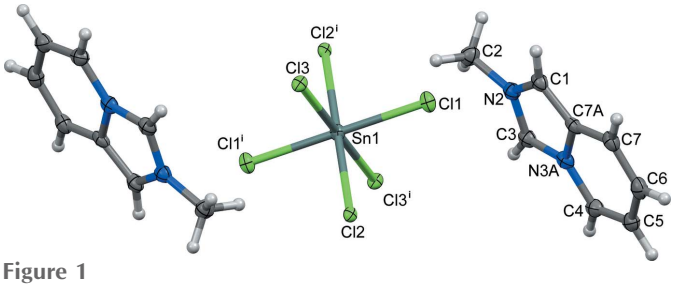

Figure 1
Molecular structure of (I) with atom labelling showing 50% displacement ellipsoids. [Symmetry code: (i) $-x+1, -y+1, -z+1$.]

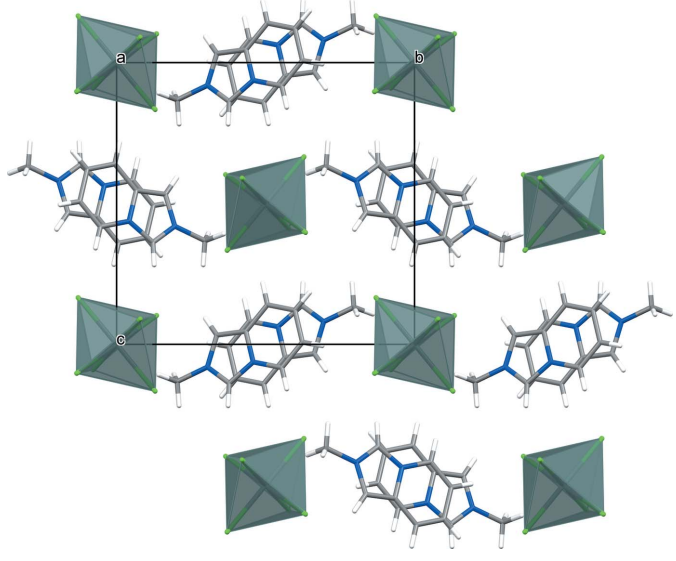

Figure 2
Projection of the crystal packing of (I) on the *bc* plane showing organic and inorganic sheets alternating parallel to the (101) plane.

Table 2
Hydrogen-bond geometry (Å, °).

D—H···A	D—H	H···A	D···A	D—H···A
C5—H5···Cl3^{ii}	0.95	2.97	3.614 (5)	126
C3—H3···Cl2^{iii}	0.95	2.65	3.549 (4)	158
C3—H3···Cl1^{iii}	0.95	2.91	3.483 (4)	120
C4—H4···Cl3^{iii}	0.95	2.96	3.473 (4)	115
C7—H7···Cl3^{iv}	0.95	2.96	3.746 (5)	141
C7—H7···Cl1^{iv}	0.95	2.91	3.605 (4)	131
C2—H2*A*···Cl1^{iii}	0.98	2.86	3.668 (5)	140
C2—H2*B*···Cl2^{v}	0.98	2.91	3.658 (5)	134
C2—H2*C*···Cl2^{i}	0.98	2.87	3.804 (4)	161
C2—H2*C*···Cl1	0.98	2.96	3.615 (4)	125

Symmetry codes: (i) $-x+1, -y+1, -z+1$; (ii) $x, y+1, z$; (iii) $x-\frac{1}{2}, -y+\frac{3}{2}, z-\frac{1}{2}$; (iv) $-x+\frac{1}{2}, y+\frac{1}{2}, -z+\frac{3}{2}$; (v) $x-1, y, z$.

3.530 (2) Å (Fig. 3). The pairs further form π-bonded chains with a distance of 3.713 (2) Å between neighbouring pyridinium ring centroids. In the anion sheet, loose packing of $SnCl_6^{2-}$ dianions that are identically stacked one above the other with the shortest Sn–Cl···Cl–Sn distance being 4.4433 (12) Å, results in a closest separation of 7.7926 (1) Å between the metal atoms. The hybrid salt lacks classical hydrogen-bonding interactions but shows a variety of C—H···Cl—Sn contacts between the organic and inorganic counterparts (Table 2), a feature common to hybrid chlorometalates with nitrogen-containing aromatic cations (Coleman *et al.*, 2013). Most of these contacts are longer than the van der Waals contact limit of 2.85 Å (Cl) (Mantina *et al.*, 2009) and can be considered a result of crystal packing.

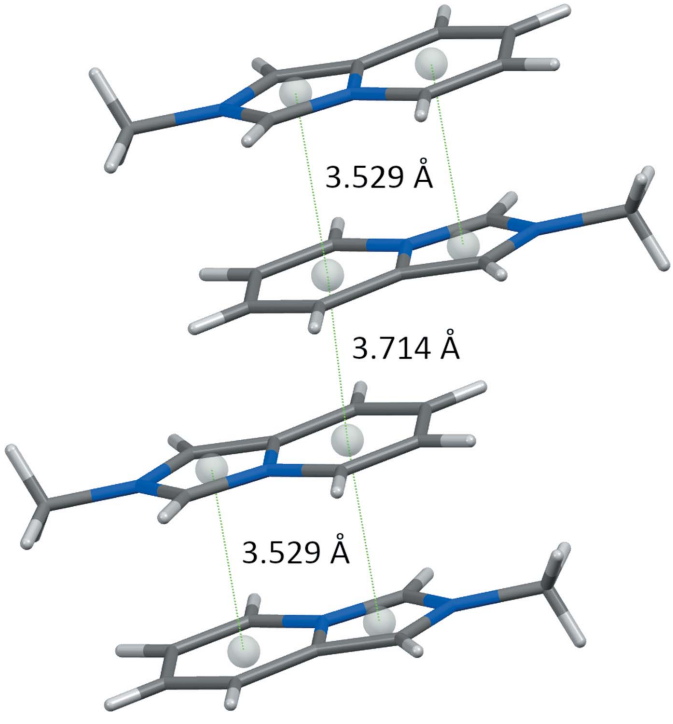

Figure 3
Fragment of the π-stacked chain built of pairs of L^+ cations of (I).

4. Database survey

A search of the Cambridge Structural Database (CSD, Version 5.42; Groom *et al.*, 2016) for structures including substituted imidazo[1,5-*a*]pyridinium cations gave 53 salts with about a half (23) reported by our research group. The latter comprise organic–inorganic hybrids with the L^+ cation or its derivatives [2-methyl-3-(pyridin-2-yl)imidazo[1,5-*a*]pyridin-2-ium and 2,2′-(ethane-1,2-diyl)bis(imidazo[1,5-*a*]pyridin-2-ium)] counterbalanced by transition and main-group (Mn, Cu, Zn, Cd, Pb) halometalates. The other compounds in the CSD with cations similar to L^+ are mostly organic salts with the imidazo[1,5-*a*]pyridinium core having various substituents in the rings. Perchlorate NAKNET (Mishra, *et al.*, 2005) and hexafluorophosphate DIWYEP (Kriechbaum, *et al.*, 2014), which bear methylphenyl and dimethylphenyl substituents, respectively, in place of the methyl group in L^+ are the most closely related. Structures of main group halometalates with substituted imidazo[1,5-*a*]pyridinium cations are limited to a few examples such as bis[2-(6-methylpyridin-2-yl)imidazo[1,5-*a*]pyridin-2-ium] dichlorogold tetrachlorogold (SUWVIR; Nandy *et al.*, 2016) and 2-(2-ammoniocyclohexyl)-3-(pyridin-2-yl)imidazo[1,5-*a*]pyridin-2-ium hexabromotellurium acetonitrile solvate (TEVVIB; Vasudevan *et al.*, 2012).

Within the variety of 279 crystal structures in the CSD comprising $[SnCl_6]^{2-}$ dianions, the latter are mostly highly symmetrical being associated with special positions. The structures including organic counterparts can be seen as an arrangement of alternating organic and inorganic layers supported by hydrogen bonds of the N–H···Cl type in the case of protonated N-containing cations. An organic–inorganic hybrid compound with the structure most similar to that of the title compound is, for example, monoclinic bis[1-(prop-2-en-1-yl)-1*H*-imidazol-3-ium] hexachloridostannate(IV), in space group $P2_1/n$, with layers formed by isolated $[SnCl_6]^{2-}$ octahedra and $(C_6H_9N_2)^+$ organic cations, which propagate along the *a*-axis direction at $y = 0$ and $y = 1/2$ (Ferjani, 2020).

5. Synthesis and crystallization

Synthesis of $[L]_2[SnCl_6]$ (I). Solid $CH_3NH_2{\cdot}HBr$ (0.45 g, 4 mmol) was added to the warm formaldehyde solution prepared by dissolving paraform (0.13 g, 4.5 mmol) in boiling deionized water (10 ml) in a 50 ml conical flask. The solution was stirred vigorously for 1 h at room temperature and filtered. On the following day, 2-PCA (0.38 ml, 4 mmol) was introduced into the flask under stirring, followed by the addition of $SnCl_2{\cdot}2H_2O$ (0.22 g, 1 mmol) dissolved in ethanol (10 ml) in 30 min. The solution was kept magnetically stirred at room temperature for another hour, then filtered to remove $Sn(OH)_2$ and allowed to evaporate. It was diluted with methanol (5 ml) since it was thickening. Pale-yellow needles of (I) suitable for X-ray crystallography formed over three months after successive addition of ^{i}PrOH (5 ml). The crystals were filtered off, washed with diethyl ether and dried in air. Yield: 12% (based on Sn). FT–IR (ν, cm^{-1}): 3422*br*, 3122*vs*, 3092*vs*, 3050*vs*, 3014, 2956, 2914, 1654, 1566, 1544, 1454, 1374,

Table 3
Experimental details.

Crystal data	
Chemical formula	$(C_8H_9N_2)_2[SnCl_6]$
M_r	597.73
Crystal system, space group	Monoclinic, $P2_1/n$
Temperature (K)	100
a, b, c (Å)	7.7926 (1), 12.1425 (1), 11.7114 (1)
β (°)	101.082 (1)
V (Å^3)	1087.49 (2)
Z	2
Radiation type	Mo $K\alpha$
μ (mm^{-1})	1.92
Crystal size (mm)	0.38 × 0.20 × 0.13
Data collection	
Diffractometer	Oxford Diffraction Gemini-R Ultra
Absorption correction	Analytical [*CrysAlis PRO* (Rigaku OD, 2016); analytical numeric absorption correction using a multifaceted crystal model based on expressions derived by Clark & Reid (1995)]
T_{min}, T_{max}	0.618, 0.802
No. of measured, independent and observed [$I > 2\sigma(I)$] reflections	18730, 2215, 2108
R_{int}	0.035
(sin $\theta/\lambda)_{max}$ (Å^{-1})	0.625
Refinement	
$R[F^2 > 2\sigma(F^2)]$, $wR(F^2)$, S	0.034, 0.098, 1.00
No. of reflections	2215
No. of parameters	125
H-atom treatment	H-atom parameters constrained
$\Delta\rho_{max}$, $\Delta\rho_{min}$ (e Å^{-3})	1.54, −1.15

Computer programs: *CrysAlis PRO* (Rigaku OD, 2016), *SHELXT2015/1* (Sheldrick, 2015*a*), *SHELXL2019/2* (Sheldrick, 2015*b*), *Mercury* (Macrae *et al.*, 2020) and *WinGX* (Farrugia, 2012).

1352, 1328, 1258, 1222, 1148vs, 1130, 1038, 986, 920, 789*vs*, 764, 742, 666, 624*vs*, 498, 468, 434. ^{1}H NMR (400 MHz, DMSO-d_6): δ (ppm) 9.83 (*s*, 1H, H_{C3}), 8.69 (*d*, 1H, J = 6.8 Hz, H_{C4}), 8.24 (*s*, 1H, H_{C1}), 7.82 (*d*, 1H, J = 9.2 Hz, H_{C7}), 7.22 (*t*, 1H, J = 8.2 Hz, H_{C5}), 7.13 (*t*, 1H, J = 6.7 Hz, H_{C6}), 4.27 (*s*, 3H, CH_3). Analysis calculated for $C_{16}H_{18}N_4SnCl_6$ (597.73): C 32.15; H 3.04; N 9.37%. Found: C 32.40; H 2.88; N 9.19%.

6. Refinement

Crystal data, data collection and structure refinement details are summarized in Table 3. All hydrogen atoms were included in calculated positions and refined using a riding model with isotropic displacement parameters based on those of the parent atom (C—H = 0.95 Å, U_{iso}(H) = 1.2U_{eq}C for CH, C—H = 0.98 Å, U_{iso}(H) = 1.5U_{eq}C for CH_3). Anisotropic displacement parameters were employed for the non-hydrogen atoms.

Funding information

Funding for this research was provided by: Ministry of Education and Science of Ukraine (project No. 22BP037-13; grant for the perspective development of the scientific direction 'Mathematical sciences and natural sciences' at the Taras Shevchenko National University of Kyiv).

References

Askar, A. M., Karmakar, A., Bernard, G. M., Ha, M., Terskikh, V. V., Wiltshire, B. D., Patel, S., Fleet, J., Shankar, K. & Michaelis, V. K. (2018). *J. Phys. Chem. Lett.* **9**, 2671–2677.
Buvaylo, E. A., Kokozay, V. N., Linnik, R. P., Vassilyeva, O. Y. & Skelton, B. W. (2015). *Dalton Trans.* **44**, 13735–13744.
Clark, R. C. & Reid, J. S. (1995). *Acta Cryst.* A**51**, 887–897.
Coleman, F., Feng, G., Murphy, R. W., Nockemann, P., Seddon, K. R. & Swadźba-Kwaśny, M. (2013). *Dalton Trans.* **42**, 5025–5035.
Farrugia, L. J. (2012). *J. Appl. Cryst.* **45**, 849–854.
Ferjani, H. (2020). *Acta Cryst.* E**76**, 1624–1628.
Gan, Z., Cheng, Y., Chen, W., Loh, K. P., Jia, B. & Wen, X. (2021). *Adv. Sci.* **8**, 2001843.
Groom, C. R., Bruno, I. J., Lightfoot, M. P. & Ward, S. C. (2016). *Acta Cryst.* B**72**, 171–179.
Kriechbaum, M., Otte, D., List, M. & Monkowius, U. (2014). *Dalton Trans.* **43**, 8781–8791.
Leblanc, A., Mercier, N., Allain, M., Dittmer, J., Pauporté, T., Fernandez, V., Boucher, F., Kepenekian, M. & Katan, C. (2019). *Appl. Mater. Interfaces*, **11**, 20743–20751.
Leijtens, T., Eperon, G. E., Noel, N. K., Habisreutinger, S. N., Petrozza, A. & Snaith, H. J. (2015). *Adv. Energy Mater.* **5**, 1500963.
Li, D., Zhang, D., Lim, K. S., Hu, Y., Rong, Y., Mei, A., Park, N. G. & Han, H. (2021). *Adv. Funct. Mater.* **31**, 2008621.
Macrae, C. F., Sovago, I., Cottrell, S. J., Galek, P. T. A., McCabe, P., Pidcock, E., Platings, M., Shields, G. P., Stevens, J. S., Towler, M. & Wood, P. A. (2020). *J. Appl. Cryst.* **53**, 226–235.
Mantina, M., Chamberlin, A. C., Valero, R., Cramer, C. J. & Truhlar, D. G. (2009). *J. Phys. Chem. A*, **113**, 5806–5812.
Mishra, D., Naskar, S., Adhikary, B., Butcher, R. J. & Chattopadhyay, S. K. (2005). *Polyhedron*, **24**, 201–208.
Nandy, A., Samanta, T., Mallick, S., Mitra, P., Seth, S. K., Saha, K. D., Al-Deyab, S. S. & Dinda, J. (2016). *New J. Chem.* **40**, 6289–6298.
Rigaku OD (2016). *CrysAlis PRO*. Rigaku Oxford Diffraction Ltd, Yarnton, England.
Rogers, R. D., Gurau, G., Kelley, S. P., Kore, R. & Shamshina, J. L. (2019). University of Alabama (UA), US Patent 10, 357, 762.
Saparov, B. & Mitzi, D. B. (2016). *Chem. Rev.* **116**, 4558–4596.
Sheldrick, G. M. (2015*a*). *Acta Cryst.* A**71**, 3–8.
Sheldrick, G. M. (2015*b*). *Acta Cryst.* C**71**, 3–8.
Sun, C., Wang, M. S. & Guo, G. C. (2019). *Appl. Mater. Interfaces*, **11**, 30713–30718.
Sun, X. Y., Yue, M., Jiang, Y. X., Zhao, C. H., Liao, Y. Y., Lei, X. W. & Yue, C. Y. (2021). *Inorg. Chem.* **60**, 1491–1498.
Vassilyeva, O. Y., Buvaylo, E. A., Kokozay, V. N. & Skelton, B. W. (2022). *Acta Cryst.* E**78**, 359–364.
Vassilyeva, O. Y., Buvaylo, E. A., Kokozay, V. N., Skelton, B. W., Rajnák, C., Titiš, J. & Boča, R. (2019). *Dalton Trans.* **48**, 11278–11284.
Vassilyeva, O. Y., Buvaylo, E. A., Linnik, R. P., Nesterov, D. S., Trachevsky, V. V. & Skelton, B. W. (2020). *CrystEngComm*, **22**, 5096–5105.
Vassilyeva, O. Y., Buvaylo, E. A., Lobko, Y. V., Linnik, R. P., Kokozay, V. N. & Skelton, B. W. (2021). *RSC Adv.* **11**, 7713–7722.
Vasudevan, K. V., Scott, B. L. & Gordon, J. C. (2012). *Main Group Chem.* **11**, 45–52.
Zhang, Y., Liu, J., Wang, Z., Xue, Y., Ou, Q., Polavarapu, L., Zheng, J., Qi, X. & Bao, Q. (2016). *Chem. Commun.* **52**, 13637–13655.

supporting information

Acta Cryst. (2023). E**79**, 103-106 [https://doi.org/10.1107/S2056989023000324]

Organic–inorganic hybrid hexachloridostannate(IV) with 2-methylimidazo[1,5-*a*]pyridin-2-ium cation

Olga Yu. Vassilyeva, Elena A. Buvaylo, Vladimir N. Kokozay and Alexandre N. Sobolev

Computing details

Data collection: *CrysAlis PRO* (Rigaku OD, 2016); cell refinement: *CrysAlis PRO* (Rigaku OD, 2016); data reduction: *CrysAlis PRO* (Rigaku OD, 2016); program(s) used to solve structure: *SHELXT2015/1* (Sheldrick, 2015a); program(s) used to refine structure: *SHELXL2019/2* (Sheldrick, 2015b); molecular graphics: *Mercury* (Macrae *et al.*, 2020); software used to prepare material for publication: *WinGX* (Farrugia, 2012).

Bis(2-methylimidazo[1,5-*a*]pyridin-2-ium) hexachloridostannate(IV)

Crystal data

$(C_8H_9N_2)_2[SnCl_6]$
M_r = 597.73
Monoclinic, $P2_1/n$
a = 7.7926 (1) Å
b = 12.1425 (1) Å
c = 11.7114 (1) Å
β = 101.082 (1)°
V = 1087.49 (2) Å^3
Z = 2
$F(000)$ = 588
D_x = 1.825 Mg m^{-3}
Mo $K\alpha$ radiation, λ = 0.71073 Å
Cell parameters from 17399 reflections
θ = 2.4–37.5°
μ = 1.92 mm^{-1}
T = 100 K
Needle, pale yellow
0.38 × 0.20 × 0.13 mm

Data collection

Oxford Diffraction Gemini-R Ultra diffractometer
Radiation source: fine-focus sealed X-ray tube, Enhance (Mo) X-ray Source
Graphite monochromator
ω scans
Absorption correction: analytical [CrysAlisPro (Rigaku OD, 2016); analytical numeric absorption correction using a multifaceted crystal model based on expressions derived by Clark & Reid (1995)]
T_{min} = 0.618, T_{max} = 0.802
18730 measured reflections
2215 independent reflections
2108 reflections with $I > 2\sigma(I)$
R_{int} = 0.035
θ_{max} = 26.4°, θ_{min} = 2.4°
h = −9→9
k = −15→15
l = −14→14

Refinement

Refinement on F^2
Least-squares matrix: full
$R[F^2 > 2\sigma(F^2)]$ = 0.034
$wR(F^2)$ = 0.098
S = 1.00
2215 reflections

125 parameters	$w = 1/[\sigma^2(F_o^2) + (0.050P)^2 + 6.970P]$
0 restraints	where $P = (F_o^2 + 2F_c^2)/3$
Hydrogen site location: inferred from neighbouring sites	$(\Delta/\sigma)_{max} < 0.001$
H-atom parameters constrained	$\Delta\rho_{max} = 1.54$ e Å^{-3}
	$\Delta\rho_{min} = -1.15$ e Å^{-3}

Special details

Geometry. All esds (except the esd in the dihedral angle between two l.s. planes) are estimated using the full covariance matrix. The cell esds are taken into account individually in the estimation of esds in distances, angles and torsion angles; correlations between esds in cell parameters are only used when they are defined by crystal symmetry. An approximate (isotropic) treatment of cell esds is used for estimating esds involving l.s. planes.

Fractional atomic coordinates and isotropic or equivalent isotropic displacement parameters (Å²)

	x	y	z	U_{iso}*/U_{eq}
Sn1	0.500000	0.500000	0.500000	0.01497 (14)
Cl1	0.35555 (12)	0.63407 (8)	0.60266 (8)	0.0195 (2)
Cl2	0.78853 (11)	0.57935 (7)	0.59047 (7)	0.01241 (19)
Cl3	0.52226 (11)	0.37088 (7)	0.66602 (7)	0.0141 (2)
C1	0.0945 (5)	0.8366 (3)	0.5329 (4)	0.0206 (8)
H1	0.048748	0.798625	0.591356	0.025*
N2	0.0816 (4)	0.8046 (3)	0.4195 (3)	0.0199 (7)
C2	−0.0015 (6)	0.7034 (4)	0.3679 (4)	0.0250 (9)
H2A	−0.023505	0.709472	0.282891	0.038*
H2B	−0.112456	0.692324	0.393919	0.038*
H2C	0.075990	0.640636	0.392353	0.038*
N3A	0.2249 (4)	0.9583 (3)	0.4373 (3)	0.0190 (7)
C3	0.1607 (5)	0.8781 (3)	0.3620 (4)	0.0206 (8)
H3	0.169920	0.874245	0.282421	0.025*
C4	0.3127 (5)	1.0545 (3)	0.4176 (4)	0.0222 (8)
H4	0.334519	1.070978	0.342328	0.027*
C5	0.3661 (5)	1.1237 (4)	0.5076 (4)	0.0232 (9)
H5	0.425896	1.189613	0.495717	0.028*
C6	0.3333 (6)	1.0986 (4)	0.6211 (4)	0.0251 (9)
H6	0.373638	1.147621	0.683721	0.030*
C7A	0.1860 (5)	0.9340 (3)	0.5465 (3)	0.0185 (8)
C7	0.2459 (6)	1.0064 (3)	0.6405 (4)	0.0214 (9)
H7	0.225017	0.990431	0.716016	0.026*

Atomic displacement parameters (Å²)

	U^{11}	U^{22}	U^{33}	U^{12}	U^{13}	U^{23}
Sn1	0.0167 (2)	0.0148 (2)	0.0133 (2)	0.00138 (12)	0.00244 (14)	0.00014 (12)
Cl1	0.0212 (5)	0.0206 (5)	0.0163 (4)	0.0061 (3)	0.0027 (3)	−0.0021 (3)
Cl2	0.0146 (4)	0.0125 (4)	0.0100 (4)	−0.0003 (3)	0.0023 (3)	−0.0006 (3)
Cl3	0.0182 (4)	0.0135 (4)	0.0104 (4)	−0.0010 (3)	0.0023 (3)	0.0003 (3)
C1	0.0206 (19)	0.021 (2)	0.0205 (19)	0.0058 (15)	0.0052 (15)	0.0039 (15)
N2	0.0186 (16)	0.0202 (17)	0.0210 (17)	0.0036 (13)	0.0041 (13)	0.0026 (13)
C2	0.024 (2)	0.023 (2)	0.027 (2)	−0.0007 (16)	0.0010 (17)	−0.0001 (17)

N3A	0.0171 (16)	0.0225 (18)	0.0173 (16)	0.0037 (13)	0.0027 (13)	0.0041 (13)
C3	0.0182 (18)	0.023 (2)	0.0201 (19)	0.0039 (15)	0.0032 (15)	0.0035 (16)
C4	0.0195 (19)	0.022 (2)	0.026 (2)	0.0030 (16)	0.0054 (16)	0.0068 (16)
C5	0.0193 (19)	0.021 (2)	0.029 (2)	0.0039 (15)	0.0043 (16)	0.0036 (17)
C6	0.023 (2)	0.025 (2)	0.027 (2)	0.0074 (17)	0.0017 (17)	−0.0025 (17)
C7A	0.0157 (18)	0.0229 (19)	0.0178 (19)	0.0077 (15)	0.0057 (14)	0.0051 (15)
C7	0.022 (2)	0.023 (2)	0.020 (2)	0.0074 (15)	0.0052 (16)	0.0010 (15)

Geometric parameters (Å, º)

Sn1—Cl1^{i}	2.4255 (9)	C2—H2C	0.9800
Sn1—Cl1	2.4255 (9)	N3A—C3	1.345 (6)
Sn1—Cl3	2.4777 (8)	N3A—C4	1.395 (5)
Sn1—Cl3^{i}	2.4778 (8)	N3A—C7A	1.401 (5)
Sn1—Cl2^{i}	2.4881 (8)	C3—H3	0.9500
Sn1—Cl2	2.4881 (8)	C4—C5	1.350 (6)
C1—N2	1.369 (5)	C4—H4	0.9500
C1—C7A	1.373 (6)	C5—C6	1.433 (6)
C1—H1	0.9500	C5—H5	0.9500
N2—C3	1.337 (5)	C6—C7	1.352 (6)
N2—C2	1.465 (5)	C6—H6	0.9500
C2—H2A	0.9800	C7A—C7	1.416 (6)
C2—H2B	0.9800	C7—H7	0.9500
Cl1^{i}—Sn1—Cl1	180.0	N2—C2—H2C	109.5
Cl1^{i}—Sn1—Cl3	89.72 (3)	H2A—C2—H2C	109.5
Cl1—Sn1—Cl3	90.28 (3)	H2B—C2—H2C	109.5
Cl1^{i}—Sn1—Cl3^{i}	90.28 (3)	C3—N3A—C4	129.1 (4)
Cl1—Sn1—Cl3^{i}	89.72 (3)	C3—N3A—C7A	109.1 (3)
Cl3—Sn1—Cl3^{i}	180.00 (2)	C4—N3A—C7A	121.8 (4)
Cl1^{i}—Sn1—Cl2^{i}	89.80 (3)	N2—C3—N3A	107.6 (4)
Cl1—Sn1—Cl2^{i}	90.20 (3)	N2—C3—H3	126.2
Cl3—Sn1—Cl2^{i}	90.59 (3)	N3A—C3—H3	126.2
Cl3^{i}—Sn1—Cl2^{i}	89.41 (3)	C5—C4—N3A	118.6 (4)
Cl1^{i}—Sn1—Cl2	90.20 (3)	C5—C4—H4	120.7
Cl1—Sn1—Cl2	89.80 (3)	N3A—C4—H4	120.7
Cl3—Sn1—Cl2	89.41 (3)	C4—C5—C6	120.6 (4)
Cl3^{i}—Sn1—Cl2	90.59 (3)	C4—C5—H5	119.7
Cl2^{i}—Sn1—Cl2	180.0	C6—C5—H5	119.7
N2—C1—C7A	107.2 (4)	C7—C6—C5	121.1 (4)
N2—C1—H1	126.4	C7—C6—H6	119.4
C7A—C1—H1	126.4	C5—C6—H6	119.4
C3—N2—C1	110.1 (4)	C1—C7A—N3A	105.9 (4)
C3—N2—C2	124.2 (4)	C1—C7A—C7	135.3 (4)
C1—N2—C2	125.7 (4)	N3A—C7A—C7	118.8 (4)
N2—C2—H2A	109.5	C6—C7—C7A	119.0 (4)
N2—C2—H2B	109.5	C6—C7—H7	120.5
H2A—C2—H2B	109.5	C7A—C7—H7	120.5

C7A—C1—N2—C3	−0.2 (4)	N2—C1—C7A—N3A	0.5 (4)
C7A—C1—N2—C2	178.1 (4)	N2—C1—C7A—C7	−178.1 (4)
C1—N2—C3—N3A	−0.2 (4)	C3—N3A—C7A—C1	−0.6 (4)
C2—N2—C3—N3A	−178.5 (3)	C4—N3A—C7A—C1	177.7 (3)
C4—N3A—C3—N2	−177.7 (4)	C3—N3A—C7A—C7	178.2 (3)
C7A—N3A—C3—N2	0.5 (4)	C4—N3A—C7A—C7	−3.4 (6)
C3—N3A—C4—C5	−179.8 (4)	C5—C6—C7—C7A	−0.1 (6)
C7A—N3A—C4—C5	2.2 (6)	C1—C7A—C7—C6	−179.2 (4)
N3A—C4—C5—C6	0.1 (6)	N3A—C7A—C7—C6	2.3 (6)
C4—C5—C6—C7	−1.1 (6)		

Symmetry code: (i) −*x*+1, −*y*+1, −*z*+1.

Hydrogen-bond geometry (Å, º)

D—H···*A*	*D*—H	H···*A*	*D*···*A*	*D*—H···*A*
C5—H5···Cl3^{ii}	0.95	2.97	3.614 (5)	126
C3—H3···Cl2^{iii}	0.95	2.65	3.549 (4)	158
C3—H3···Cl1^{iii}	0.95	2.91	3.483 (4)	120
C4—H4···Cl3^{iii}	0.95	2.96	3.473 (4)	115
C7—H7···Cl3^{iv}	0.95	2.96	3.746 (5)	141
C7—H7···Cl1^{iv}	0.95	2.91	3.605 (4)	131
C2—H2*A*···Cl1^{iii}	0.98	2.86	3.668 (5)	140
C2—H2*B*···Cl2^{v}	0.98	2.91	3.658 (5)	134
C2—H2*C*···Cl2^{i}	0.98	2.87	3.804 (4)	161
C2—H2*C*···Cl1	0.98	2.96	3.615 (4)	125

Symmetry codes: (i) −*x*+1, −*y*+1, −*z*+1; (ii) *x*, *y*+1, *z*; (iii) *x*−1/2, −*y*+3/2, *z*−1/2; (iv) −*x*+1/2, *y*+1/2, −*z*+3/2; (v) *x*−1, *y*, *z*.